Article

TRANSPARENT PROCESS

THE EMBO JOURNAL

Shelterin promotes tethering of late replication origins to telomeres for replication-timing control

Shiho Ogawa[1], Sayuri Kido[1], Tetsuya Handa[1,†], Hidesato Ogawa[2], Haruhiko Asakawa[2], Tatsuro S Takahashi[1,‡], Takuro Nakagawa[1], Yasushi Hiraoka[2] & Hisao Masukata[1,2,*]

Abstract

DNA replication initiates at many discrete loci on eukaryotic chromosomes, and individual replication origins are regulated under a spatiotemporal program. However, the underlying mechanisms of this regulation remain largely unknown. In the fission yeast *Schizosaccharomyces pombe*, the telomere-binding protein Taz1, ortholog of human TRF1/TRF2, regulates a subset of late replication origins by binding to the telomere-like sequence near the origins. Here, we showed using a *lacO*/LacI-GFP system that Taz1-dependent late origins were predominantly localized at the nuclear periphery throughout interphase, and were localized adjacent to the telomeres in the G1/S phase. The peripheral localization that depended on the nuclear membrane protein Bqt4 was not necessary for telomeric association and replication-timing control of the replication origins. Interestingly, the shelterin components Rap1 and Poz1 were required for replication-timing control and telomeric association of Taz1-dependent late origins, and this requirement was bypassed by a minishelterin Tpz1-Taz1 fusion protein. Our results suggest that Taz1 suppresses replication initiation through shelterin-mediated telomeric association of the origins at the onset of S phase.

Keywords chromatin organization; Rap1; replication timing; Taz1; telomere
Subject Categories Chromatin, Epigenetics, Genomics & Functional Genomics; DNA Replication, Repair & Recombination
DOI 10.15252/embj.201898997 | Received 10 January 2018 | Revised 19 May 2018 | Accepted 19 June 2018 | Published online 11 July 2018
The EMBO Journal (2018) 37: e98997

Introduction

To ensure complete duplication of the eukaryotic genome within the S phase of the cell cycle, DNA replication initiates from a number of discrete loci known as replication origins. Replication at these origins is not initiated simultaneously at the beginning of S phase, but rather at distinct origin-specific times during S phase. Temporal control of replication is conserved from yeasts to metazoans (MacAlpine & Bell, 2005; Gilbert *et al*, 2010).

In mammalian cells, replication foci characteristic of actively replicating chromosomal regions are localized to the interior of the nucleus in early S phase, while they are localized to the nuclear periphery from mid to late S phase (Nakamura *et al*, 1986; Nakayasu & Berezney, 1989; O'Keefe *et al*, 1992). Prior studies suggest that a spatiotemporal replication program is established at a specific time point (timing decision point, TDP) in the G1 phase (Dimitrova & Gilbert, 1999). In budding yeast, late replication origins are localized proximal to the nuclear envelope in G1-arrested cells, while early origins are randomly distributed within the nucleus (Heun *et al*, 2001). However, artificial tethering of an early replication origin to the nuclear membrane did not shift its replication timing to late S phase, suggesting that peripheral localization of origins *per se* is not the critical determinant for their activation timing (Ebrahimi *et al*, 2010). Therefore, the molecular mechanisms of spatiotemporal replication control remain largely elusive.

Telomeres are specialized chromatin structures composed of an array of short telomeric repeats and specific binding proteins at the end of linear chromosomes in eukaryotes. In *Schizosaccharomyces pombe*, the telomeric protein Taz1 directly binds to double-stranded telomere DNA (Cooper *et al*, 1997; Spink *et al*, 2000) and recruits two proteins, Rap1 and Rif1, to the telomeres (Kanoh & Ishikawa, 2001). Taz1 and Rap1, together with other components including Poz1, Tpz1, Ccq1, and Pot1, form the conserved shelterin complex that protects telomere ends and controls telomere length (Miyoshi *et al*, 2008; Palm & de Lange, 2008). Telomeres are anchored to the nuclear periphery through redundant mechanisms in many organisms (Palladino *et al*, 1993; Chikashige *et al*, 2009; Crabbe *et al*, 2012; Ferreira *et al*, 2013). In *S. pombe*, telomeres are clustered together and anchored to the nuclear periphery through the interaction of Rap1 with the nuclear membrane proteins Bqt3 and Bqt4 (Chikashige *et al*, 2009). Telomere clustering is required for meiotic chromosome movement and homologous recombination (Chikashige *et al*, 2006), but not for telomere length control or heterochromatin formation in the mitotic cell cycle (Chikashige *et al*, 2010).

Recent studies have demonstrated that telomere-binding proteins play crucial roles in replication-timing control in *S. pombe*. A subset

1 Graduate School of Science, Osaka University, Toyonaka, Osaka, Japan
2 Graduate School of Frontier Biosciences, Osaka University, Suita, Osaka, Japan
*Corresponding author. Tel: +81 6 6850 5432; Fax: +81 6 6850 5440; E-mail: masukata@bio.sci.osaka-u.ac.jp
†Present address: Cell Biology Center, Institute of Innovative Research, Tokyo Institute of Technology, Yokohama, Kanagawa, Japan
‡Present address: Faculty of Science, Kyushu University, Fukuoka, Japan

of late-replicating origins are accompanied by two copies of a telomere-like sequence, and binding of Taz1 to this sequence is essential for the late-timing control of these origins (Tazumi *et al*, 2012). In addition, these Taz1-dependent late origins require Rif1 for timing regulation, although Rif1 is not localized to the origins (Hayano *et al*, 2012; Tazumi *et al*, 2012; Kanoh *et al*, 2015). Both Taz1 and Rif1 are also required for regulation of the late origins in subtelomeres spanning as far as 100 kb from the chromosome ends (Tazumi *et al*, 2012). However, Rif1 regulates another type of late origin, where Rif1 is localized independently of Taz1 (Hayano *et al*, 2012; Tazumi *et al*, 2012; Kanoh *et al*, 2015).

Recently, an intriguing model has been proposed in which Rif1 recruits protein phosphatase 1 (PP1) that acts as a counter-phosphatase against the phosphorylation of Mcm2-7 subunits (Dave *et al*, 2014; Hiraga *et al*, 2014; Mattarocci *et al*, 2014). Because phosphorylation of Mcm2 and Mcm4 by Dbf4-dependent kinase (DDK) is essential for the assembly of initiation factors including Sld3, GINS, and Cdc45, recruitment of PP1 to the replication origins prevents replication initiation at the onset of S phase. This model is consistent with regulation of the subtelomeric origins and Taz1-independent late origins, where Rif1 is localized. However, it is unclear whether replication-timing control of Taz1-dependent late origins, where Rif1 is not localized, involves additional mechanisms such as localization to specific intra-nuclear regions where Rif1 and PP1 are abundant.

Here, we used a fluorescence microscopy system to examine whether replication origins, especially the Taz1-dependent late origins, were localized to specific intra-nuclear compartments in living fission yeast cells. The Taz1-dependent late origins were localized adjacent to telomeres at the nuclear periphery during G1/S phase. Interestingly, the shelterin components Rap1 and Poz1 were required for replication-timing control as well as telomeric association of the Taz1-dependent late origins located in chromosomal arm regions, although these components were dispensable for the timing control of subtelomeric late origins. Moreover, expression of a minishelterin Tpz1-Taz1 fusion protein restored both replication-timing control and telomeric association of the origins in *rap1*Δ *poz1*Δ cells. These results suggest that Taz1 regulates the late replication timing of inner arm origins through shelterin-mediated telomere association in *S. pombe*.

Results

Distinct intra-nuclear localizations of early and late replication origins

To visualize the subnuclear localization of early and late replication origins in *S. pombe*, the replication origins were tagged with a *lacO* array/GFP-conjugated LacI repressor. A *lacO* array of approximately 10 kb was inserted at 0.1 kb from the well-characterized early origin *ars2004*, or at 0.7 kb from the Taz1-dependent late origin *AT2088* located on the left or right arm, respectively, of chromosome II (Fig 1A). Insertion of the *lacO* array did not change the replication timing of either origin (Appendix Fig S1).

Localization of the LacI-GFP-tagged origin relative to mCherry-fused Ish1, a nuclear envelope protein (Taricani *et al*, 2002), was analyzed in living cells under a fluorescence microscope. Among 21 focal planes, we selected a single plane that contained the strongest LacI-GFP signal (Fig 1B). Interestingly, the *AT2088*-LacI-GFP focus colocalized with Ish1-mCherry at the nuclear membrane, whereas *ars2004*-LacI-GFP was observed at various locations in the nucleus (Fig 1C). For a quantitative analysis of LacI-GFP localization in the nucleus, the number of cells with Ish1-mCherry colocalization (peripheral, Class 1) and those without colocalization (non-peripheral, Class 2) were counted (Fig 1D). The proportion of Class 1 was 79.3% for *AT2088*-LacI-GFP, and 48.5% for *ars2004*-LacI-GFP (Fig 1D). The difference in intra-nuclear localization of the two origins was statistically significant ($P < 0.0001$, Fisher's exact test). These results demonstrate that *AT2088* is more predominantly located at the nuclear periphery than *ars2004*.

We then examined whether peripheral localization is a common property of late replication origins. Another Taz1-dependent late origin, *ori2100*, which is located near the centromere on the right arm of chromosome II (Fig 1A), predominantly colocalized with Ish1-mCherry on the nuclear membrane, similar to *AT2088* ($P > 0.9999$; Fig 1E and Appendix Fig S2). In contrast, a different type of late origin, *ars727*, which is dependent on Rif1 but not Taz1 and located on the right arm of chromosome II (Fig 1A), had 57.4% Class 1 localization, which was statistically different from that of *AT2088* and *ori2100* (*P*-values < 0.0001; Fig 1E and Appendix Fig S2). In addition, the early origins *ori2024* and *ori2123* (Fig 1A) did

Figure 1. Taz1-dependent late replication origins are localized at the nuclear periphery.

A The locations of early and late replication origins relevant to this study are schematically shown on *Schizosaccharomyces pombe* chromosome II. The early origins *ars2004*, *ori2024*, and *ori2123*, the Taz1-dependent late origins *AT2088* and *ori2100*, and the Taz1-independent late origin *ars727* are indicated. The location of the centromere (*cen2*) is depicted by a yellow square, and the telomeres are indicated by black arrowheads.

B Schematic images for the analysis of the subnuclear locations of LacI-GFP-tagged replication origins in comparison with the mCherry-Ish1 at the nuclear envelope under a fluorescence microscope. Among 21 focal planes with 0.1-μm focus intervals, a single plane that contained the strongest *lacO*/LacI-GFP signal was chosen for quantitative analyses.

C Representative images of *lacO*/LacI-GFP (green) at the *AT2088* late origin (upper 4 panels) and at the *ars2004* early origin (lower 4 panels) merged with Ish1-mCherry (red) are presented. The optical section images were processed as described in "Materials and Methods". The scale bar indicates 5 μm.

D Images were classified into two categories: Class 1 (peripheral), GFP signals that overlapped with Ish1-mCherry; and Class 2 (non-peripheral), GFP signals that did not overlap with or had separated from Ish1-mCherry. The proportions of Class 1 (blue) and Class 2 (pale blue) of the *AT2088* late origin and the *ars2004* early origin are presented in pie charts.

E The Class 1 and Class 2 proportions of *ori2100* (Taz1-dependent late origin), *ars727* (Taz1-independent late origin), *ori2024* (early origin), and *ori2123* (early origin) are shown in pie charts.

F The effect of a base substitution (*AT2088-S2632*) in the telomere-like sequence near the *AT2088* on the peripheral localization of *AT2088* and the effects of deletion of *taz1*$^+$ on the localizations of late origins *AT2088* and *ori2100*, and the early origin *ars2004* were examined. Representative images of *lacO*/LacI-GFP (green) and Ish1-mCherry (red) are presented with the proportions of Class 1 (peripheral, blue) and Class 2 (non-peripheral, pale blue). The scale bar indicates 5 μm.

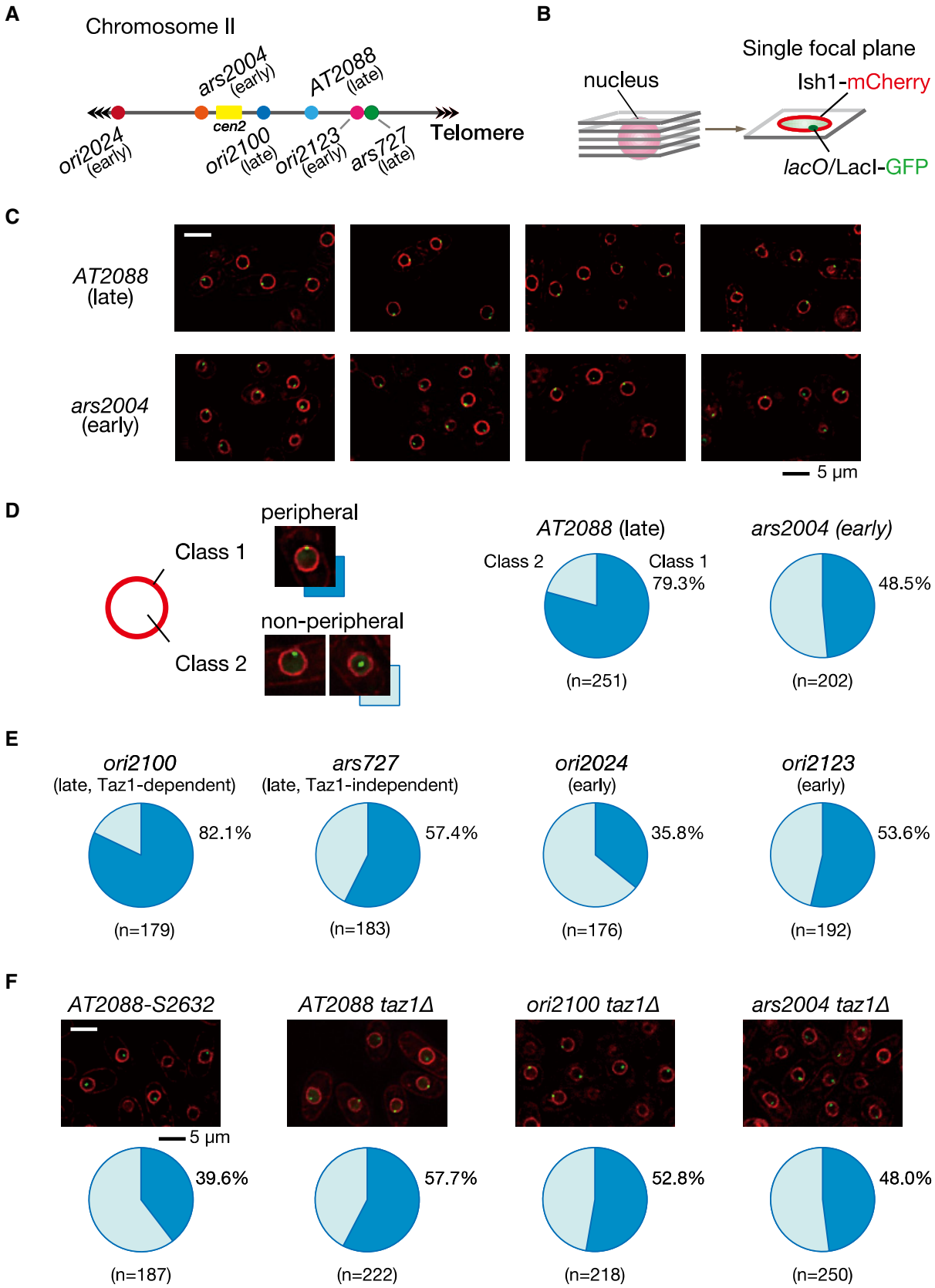

Figure 1.

not exhibit preferential localization at the nuclear periphery compared to *AT2088* (P-values < 0.0001; Fig 1E and Appendix Fig S2). The localization pattern of each origin was not significantly altered between the G1/S and G2 phases (Fig EV1). However, the results of a time-lapse analysis suggested that the Taz1-dependent late origin *AT2088* dissociated from the nuclear periphery during the M phase (Fig EV2). Therefore, our results show that Taz1-dependent late origins localize at the nuclear periphery throughout the interphase of the cell cycle at a higher frequency than Taz1-independent late origins and early origins.

Late replication origins are localized to the nuclear periphery through a Taz1-dependent mechanism

Because only Taz1-dependent late origins exhibited preferential localization at the nuclear periphery, we sought to determine whether regulation of localization involved a Taz1-dependent mechanism. We first examined whether the telomere-like sequence, the Taz1-binding site, which is located proximal to *AT2088* and essential for replication-timing control (Tazumi *et al*, 2012), was required for peripheral localization of the origin by generating a mutant for this sequence. The *AT2088-S2632* substitution in the telomere-like sequence markedly decreased the Class 1 proportion from 79.3 to 39.6% (Fig 1F, P < 0.0001 compared to *AT2088*), indicating that the telomere-like sequence is essential for the peripheral localization of the origin. Next, we examined whether Taz1 was required for the nuclear peripheral localization of Taz1-dependent late origins. The Class 1 proportion of *AT2088* decreased from 79.3% in wild-type cells to 57.7% in *taz1*Δ cells (Fig 1F, P < 0.0001). The Class 1 proportion of another Taz1-dependent late origin, *ori2100*, also decreased in *taz1*Δ cells (P < 0.0001 compared to *ori2100* in wild-type cells), whereas the localization of the early origin *ars2004* did not significantly change (P = 0.91, compared to *ars2004* in wild-type cells; Fig 1F). These results indicate that Taz1 binding near the origin is required for the nuclear peripheral localization of Taz1-dependent late origins.

AT2088 occupies a telomere-adjacent location during G1/S phase

Because the telomeres are anchored to the inner nuclear membrane during the interphase of the mitotic cell cycle (Chikashige *et al*, 2009), we asked if Taz1-dependent late origins could associate with telomeres in the nuclear periphery. To test this possibility, we analyzed the location of *AT2088*-LacI-GFP in comparison with that of Taz1-mCherry (Fig 2A). In a single focal plane, which was selected based on the strongest LacI-GFP signal, one to four Taz1-mCherry foci, which corresponded to the telomeres of chromosomes I and II, were detected (Fig 2B). In some nuclei, the *AT2088*-LacI-GFP focus was close to or partially overlapped with one of the Taz1-mCherry foci, generating yellow boundary in the merged image (Fig 2B and C).

For a more detailed investigation of how these localizations corresponded to the cell cycle, we took advantage of the *S. pombe* morphology, in which G1/S phase and G2 phase cells correspond to bi-nuclear and single-nuclear cells, respectively, because cytokinesis and septum formation coincide with the G1/S phase. We measured the distance between the LacI-GFP focus and the closest Taz1-mCherry focus in G1/S and G2 phase cells (Fig 2A and D). Interestingly, the distance was significantly smaller in G1/S phase cells than in G2 phase cells (P < 0.0001, Kruskal–Wallis test, Fig 2D). The results of time-lapse analysis further suggested that *AT2088*-LacI-GFP locus began to associate with the telomere shortly after sister chromatids separated in the M phase, and it moved within the vicinity of the telomere through G1/S phase (Fig EV3). Taken together, the *AT2088* locus associates with the telomere from late M phase to G1/S phase, and it separates from the telomere in G2 phase although both *AT2088* and the telomeres remain at the nuclear periphery (Fig 2E).

To examine whether the telomere-adjacent localization of *AT2088* was regulated by a Taz1-dependent mechanism, the effect of a base substitution in the telomere-like sequence near *AT2088* was analyzed. The distance between *AT2088-S2632*-LacI-GFP and the closest Taz1-mCherry focus in G1/S phase increased compared to that in wild-type cells (Fig 2D, P < 0.0001, Kruskal–Wallis test), and there was no significant difference between G1/S and G2 phases in *AT2088-S2632* cells (Fig 2D, P = 0.40). These results suggest that telomeric association of Taz1-dependent late origins requires Taz1 binding to telomere-like sequences near the origins.

Telomeric association and replication-timing control of Taz1-dependent late origins are independent of nuclear peripheral localization

Telomeres are anchored to the inner nuclear membrane in the mitotic cell cycle through the interaction of Rap1 with nuclear membrane proteins Bqt3/4 (Chikashige *et al*, 2009). To examine whether anchoring of telomeres to the nuclear membrane played a role in telomeric association of Taz1-dependent late origin, we analyzed the nuclear localization of *AT2088*-LacI-GFP in comparison with that of Taz1-mCherry in *bqt4*Δ cells. Taz1-mCherry foci were found in the interior of the nucleus in *bqt4*Δ cells (Fig 3A), consistent with previous observations (Chikashige *et al*, 2009). Interestingly, *AT2088*-LacI-GFP was located in close proximity to one of the interiorly shifted telomeres in *bqt4*Δ cells (Fig 3A). The distance between the *AT2088*-LacI-GFP signal and the closest Taz1-mCherry focus of *bqt4*Δ cells was significantly smaller in G1/S phase than in G2 phase (Fig 3B, P = 0.0027, Kruskal–Wallis test) and was similar to that in wild-type G1/S phase cells (Fig 3B, P > 0.9999). These results suggest that the telomeric localization of Taz1-dependent late origins is independent of telomere anchoring to the inner nuclear membrane.

Because *AT2088* remained in close association with telomeres that changed location toward the interior of the nucleus in *bqt4*Δ cells, we examined whether the location of the origin relative to Ish1-mCherry was altered (Fig 3C). The proportion of *AT2088* Class 1 localization remarkably decreased in G1/S and G2 phases in *bqt4*Δ cells (Fig 3C, P < 0.0001 compared to wild-type cells). Similarly, the Class 1 localization of *ori2100* decreased in *bqt4*Δ cells (Appendix Fig S3), indicating that peripheral localization of Taz1-dependent origins was dependent on Bqt4. Taken together, these results demonstrate that peripheral localization is not a prerequisite for the association between telomeres and Taz1-dependent late origins.

To examine whether the peripheral localization of Taz1-dependent origins is required for late replication-timing control in

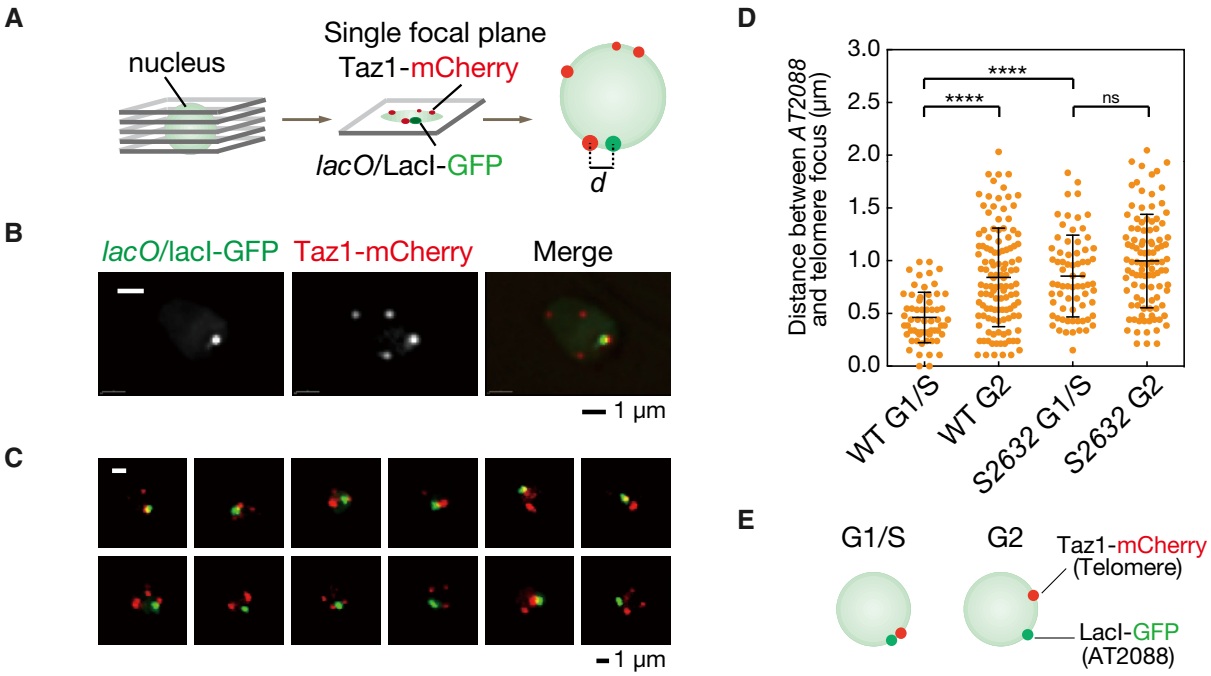

Figure 2. G1/S phase-specific telomeric association of late origin *AT2088*.

A Schematic images are shown for the analysis of the location of *AT2088*-LacI-GFP in comparison with Taz1-mCherry at the telomeres. Among 21 vertical planes with 0.1-μm intervals, a single plane that contained both a strong *lacO*/LacI-GFP (green) signal and the closest Taz1-mCherry (red) signal is chosen for analysis. For quantitative analysis of the locations of *AT2088* locus in comparison with telomeres, the distance between the center of *AT2088*-LacI-GFP signal and that of the closest Taz1-mCherry signal (telomere) in a single focal plane was measured.

B The LacI-GFP signal at *AT2088* (left), the Taz1-mCherry foci at the telomeres (middle), and the merged image (right) in a single focal plane are presented. The scale bar indicates 1 μm.

C Merged images of LacI-GFP and Taz1-mCherry are presented as in (B). The scale bar indicates 1 μm.

D The distances between the center of *AT2088*-LacI-GFP signal and that of the closest Taz1-mCherry signal (telomere) were measured in a single focal plane in G1/S and G2 phase nuclei of wild-type and *AT2088-S2632* cells (as in A). The results (μm) are presented in the scatter plot. Lines indicate means ± SD. The numbers of nuclei analyzed were n = 60 and n = 119 for G1/S and G2 phases in wild type, respectively, and n = 70 and n = 103 for G1/S and G2 phases in *AT2088-S2632* cells, respectively. *P*-values were calculated using the Kruskal–Wallis test in GraphPad Prism 6. ****$P < 0.0001$.

E Schematic drawings of the *lacO*/LacI-GFP (*AT2088*) and Taz1-mCherry (telomere) in G1/S and G2 phases based on the results of Figs 1 and 2 are presented.

S. pombe, we measured DNA synthesis in wild-type and *bqt4*Δ cells in the presence of hydroxyurea (HU), an inhibitor of ribonucleotide reductase, which prevents replication fork progression and late origin activation. Wild-type and *bqt4*Δ cells were arrested at the G2/M boundary and then synchronously released and labeled with 5-bromo-2′-deoxyuridine (BrdU), a heavy-density analog of thymidine. BrdU-labeled heavy-light density DNA was separated from non-replicated light–light density DNA by CsCl density gradient centrifugation, and DNA replication (%) was quantified by qPCR as described previously (Hayashi *et al*, 2007). In HU-treated wild-type cells, the early origin *ars2004* incorporated BrdU several times more than a non-origin locus (nonARS), late replication origins *ori2100* and *AT2088*, or the subtelomeric late origin *TAS59* (Fig 3D), consistent with previous results (Tazumi *et al*, 2012). In *bqt4*Δ cells, the replication profile, in which early replication occurred only at *ars2004* but not at *ori2100*, *AT2088* or *TAS59*, was very similar to that in wild-type cells (Fig 3D), demonstrating that Bqt4 does not play a role in replication-timing control. Therefore, nuclear peripheral localization is not a crucial determinant for replication timing of Taz1-dependent late origins and subtelomeric late origins.

Shelterin components play important roles in replication-timing control and telomeric association of Taz1-dependent late origins

We then investigated whether other telomere-binding proteins, such as shelterin components, participated in replication-timing control and telomeric association of late origins. To examine the role of Rap1 in replication-timing control, BrdU incorporation was measured for the early origin *ars2004*, the Taz1-dependent late origins *AT2088* and *ori2100*, the Taz1-independent late origin *ars727*, and the subtelomeric late origins *TAS59* and *tel-0.3* (Fig 4A). In HU-treated wild-type cells, all of the late origins and the non-origin region (nonARS) did not significantly replicate, while the early origin *ars2004* replicated early (Fig 4A). Contrastingly, in HU-treated *taz1*Δ cells, *ori2100*, *AT2088*, *TAS59*, and *tel-0.3* replicated to a similar extent of *ars2004*, whereas replication of *ars727*, the Taz1-independent late origin, remained lower than that of the nonARS control (Fig 4A), consistent with previous findings (Tazumi *et al*, 2012). Replication at the nonARS in *taz1*Δ cells was higher than that in wild-type cells, possibly due to passive replication from a weak Taz1-dependent origin located about 15 kb from the locus. Interestingly, in HU-treated *rap1*Δ

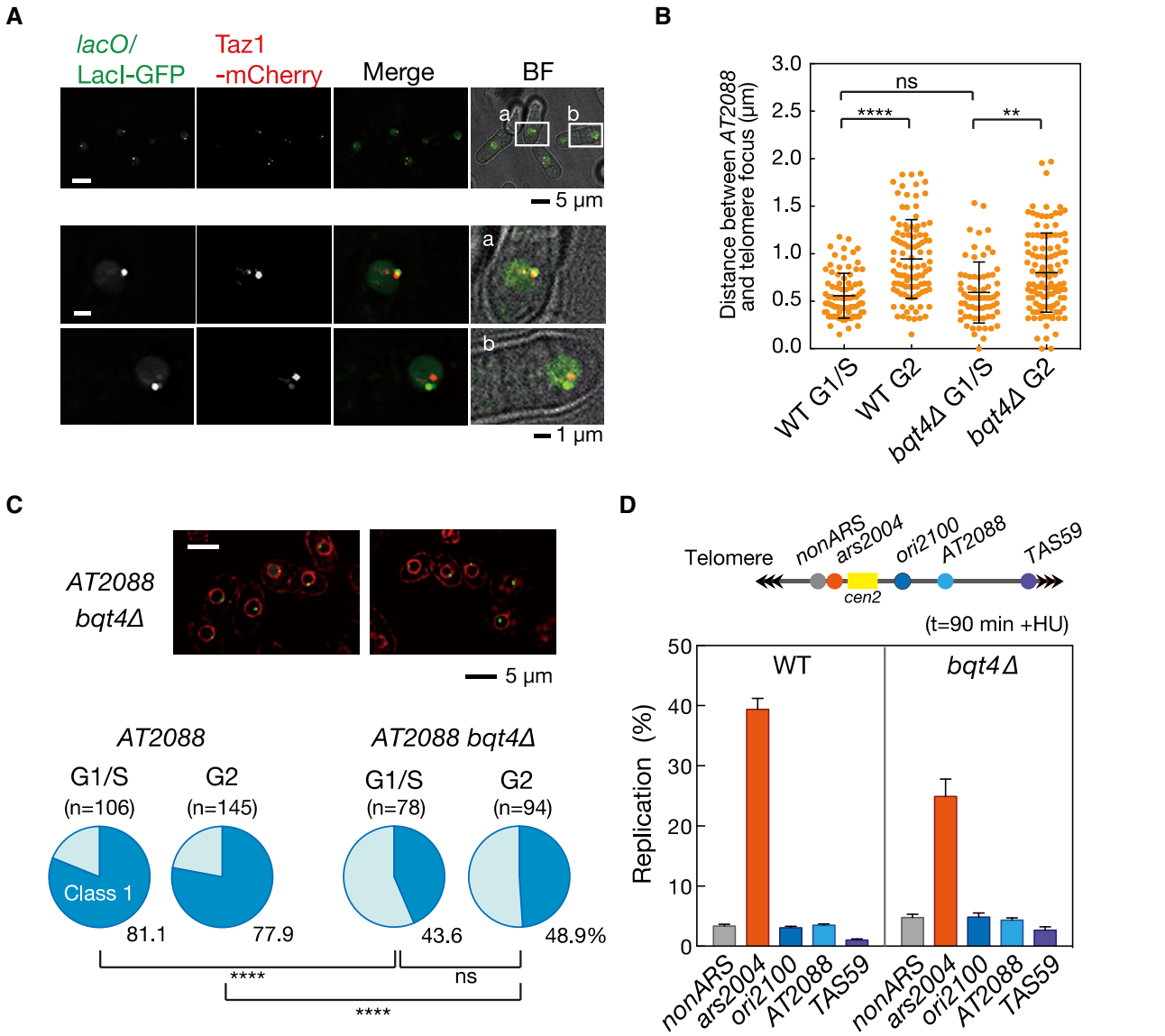

Figure 3. Telomere anchoring to the nuclear membrane is not required for telomeric association of the Taz1-dependent origin and late replication control.

A Localization of *AT2088*-LacI-GFP in comparison with Taz1-mCherry was analyzed in *bqt4*Δ cells. Representative images of a single focal section (top) with enlarged images for the regions "a" (middle) and "b" (bottom) in G1/S phase cells are shown. One of the two nuclei in the G1/S phase cell containing "a" is out of focus. The scale bar indicates 5 μm (top panels) or 1 μm (middle and bottom panels).

B The distances between the *AT2088*-LacI-GFP focus and the closest Taz1-mCherry in G1/S (n = 85) and G2 (n = 101) phases of wild-type cells and G1/S (n = 68) and G2 (n = 112) phases of *bqt4*Δ cells are shown in the scatter plots. Lines indicate means ± SD. *P*-values were calculated using the Kruskal–Wallis test. ****$P < 0.0001$ and **$P < 0.01$.

C Representative images of *lacO*/LacI-GFP (green) at the *AT2088* merged with Ish1-mCherry (red) in *bqt4*Δ cells are presented. The proportions of Class 1 (peripheral, blue) and Class 2 (non-peripheral, pale blue) during G1/S and G2 phases of *bqt4*Δ cells together with the results of wild type (as shown in Fig EV1) are shown in the pie charts. *P*-values were obtained using the Fisher's exact test. ****$P < 0.0001$.

D Effect of *bqt4*$^+$ deletion on replication timing of early and late origins. Wild-type and *bqt4*Δ cells synchronously released from the G2/M block were labeled with BrdU for 90 min at 25°C in the presence of HU. Replication (%) was quantified as described in "Materials and Methods" by qPCR using primers for *nonARS*, early origin *ars2004*, late origins *ori2100* and *AT2088*, and subtelomeric origin *TAS59*. The mean values obtained from three independent experiments are presented ±SEM.

cells, the Taz1-dependent late origins *AT2088* and *ori2100* showed early replication, whereas subtelomeric *TAS59* and *tel-0.3* and *ars727* showed late replication as observed in wild-type cells (Fig 4A). Furthermore, in *poz1*Δ cells lacking another component of the shelterin complex, the results were very similar to those in *rap1*Δ cells (Fig 4A), indicating that Rap1 and Poz1 are required for the timing control of the Taz1-dependent origins. These results show that Rap1 and Poz1 are required specifically for replication-timing control of Taz1-dependent origins located in the chromosomal arm regions, but are dispensable for control of telomere-proximal origins and the Taz1-independent late origin.

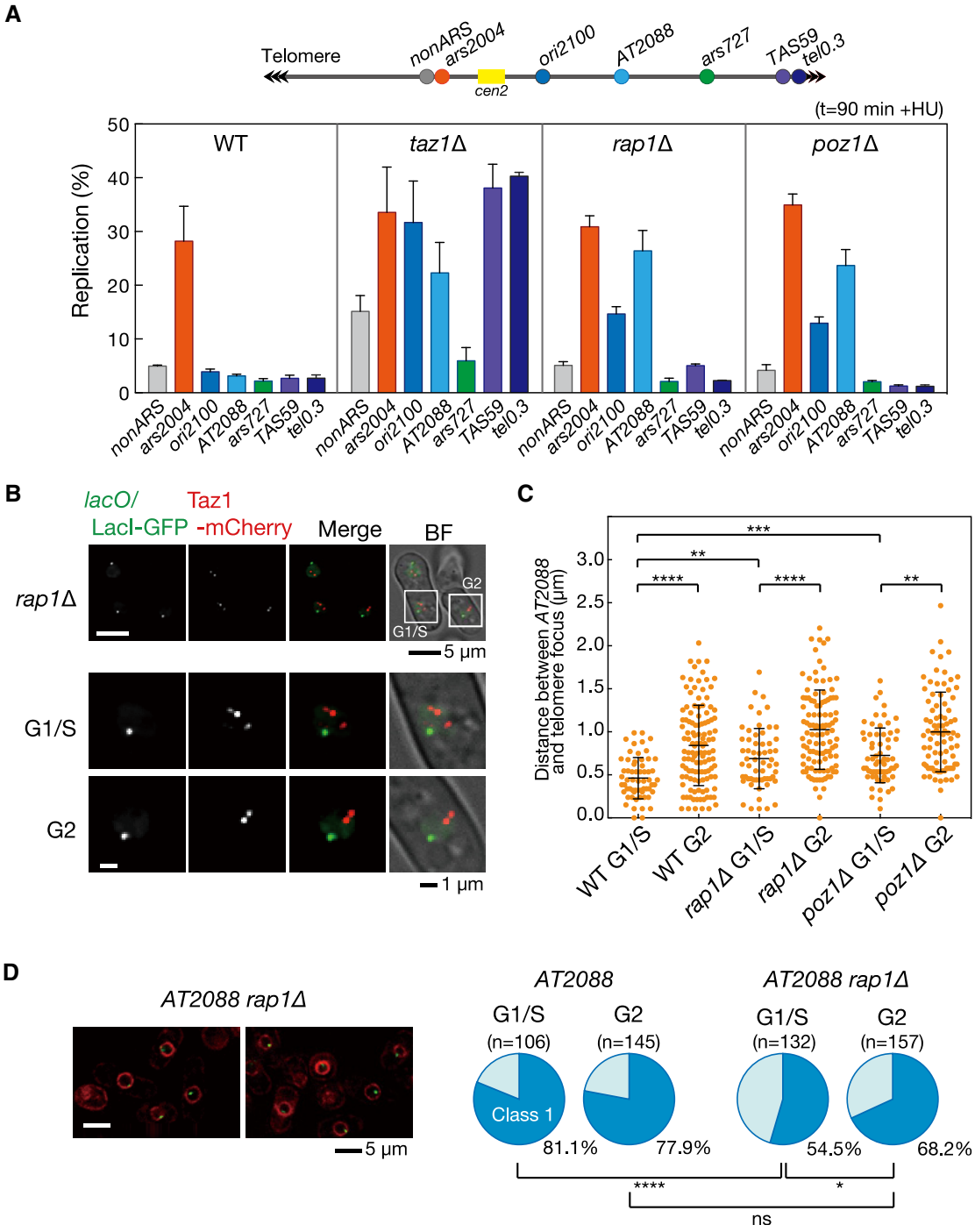

Figure 4. Shelterin components Rap1 and Poz1 are required for replication-timing control and telomeric association of Taz1-dependent late origins.

A Effects of shelterin component deletion on replication timing of late origins. Wild-type, *taz1*Δ, *rap1*Δ, and *poz1*Δ cells were synchronously released from the G2/M block and labeled with BrdU for 90 min in the presence of HU. Replication (%) was analyzed as described in Fig 3. The mean values obtained from three independent experiments are presented ±SEM.

B Localization of *AT2088*-LacI-GFP in comparison with Taz1-mCherry was analyzed in *rap1*Δ cells. Representative images of a single focal section (top) with enlarged images for the regions "G1/S" (middle) and "G2" (bottom) are shown. The scale bar indicates 5 μm (top panels) or 1 μm (middle and bottom panels).

C Distances between the *AT2088*-LacI-GFP focus and the closest Taz1-mCherry (telomere) during G1/S (n = 60) and G2 (n = 108) phases of *rap1*Δ cells and G1/S (n = 64) and G2 (n = 86) phases of *poz1*Δ cells together with the results of wild-type cells (as in Fig 2) are shown in the scatter plots. Lines indicate means ± SD. P-values were obtained by the Kruskal–Wallis test. ****P < 0.0001, ***P < 0.001, and **P < 0.01.

D Representative images of *lacO*/LacI-GFP (green) at the *AT2088* merged with Ish1-mCherry (red) in *rap1*Δ cells. Class 1 (peripheral) and Class 2 (non-peripheral) proportions in G1/S and G2 phases *rap1*Δ cells together with the results of wild type (as shown in Fig EV1) are shown in pie charts. P-values were calculated using Fisher's exact test. ****P < 0.0001 and *P < 0.05.

Because Taz1 binding to the telomere-like sequence near the internal late origins is essential for late-timing control of the origins, we examined the localization of Taz1 to the *AT2088* locus in wild-type and *rap1*Δ cells. A chromatin immunoprecipitation (ChIP) assay using Flag-Taz1 showed that the amount of Flag-Taz1 localized to the *AT2088* locus in *rap1*Δ cells was similar to that in wild-type cells (Fig EV4). We then examined whether Rap1 was localized at the *AT2088* locus to affect replication timing. The results of ChIP analysis with Rap1-Flag showed that there was no significant localization of Rap1-Flag at the *AT2088* locus in comparison with the control locus (nonARS) at the G2/M boundary or in G1/S phase, although Rap1-Flag was localized to the region close to the telomeres (Fig EV5). Thus, it is likely that Rap1 plays a role in replication-timing control of *AT2088* without stable localization at the locus.

We examined whether Rap1 or Poz1 are involved in the intra-nuclear localization of Taz1-dependent late origins. In the absence of Rap1, Taz1-mCherry foci shifted toward the interior of the nucleus, as was observed in *bqt4*Δ cells (Fig 4B). This was consistent with the requirement of Rap1 for telomere anchoring to the inner nuclear membrane. In contrast to the results in *bqt4*Δ cells, the *AT2088*-LacI-GFP focus was located distant from Taz1-mCherry foci (Fig 4B). The distance between *AT2088*-LacI-GFP and the closest Taz1-mCherry focus in G1/S phase of *rap1*Δ cells was significantly larger than in wild-type cells (Fig 4C, $P = 0.0064$, Kruskal–Wallis test), although the distance was smaller than in G2 phase *rap1*Δ cells (Fig 4C, $P < 0.0001$). These results suggest that Rap1 has a role, at least in part, in the close association of the origin with telomeres. Similarly, in *poz1*Δ cells, the distance between *AT2088*-LacI-GFP and the closest Taz1-mCherry focus in G1/S phase cells increased compared to that in wild-type cells (Fig 4C, $P = 0.0004$ and Appendix Fig S4). Intriguingly, the proportion of peripheral *AT2088* (Class 1) localization in *rap1*Δ G1/S phase cells decreased compared to that in wild-type cells (Fig 4D, $P < 0.0001$, Fisher's exact test) and was significantly smaller than in G2 phase *rap1*Δ cells (Fig 4D, $P = 0.021$). These results suggest that the shelterin components Rap1 and Poz1 have roles in the intra-nuclear localization of Taz1-dependent late origins primarily during G1/S phase.

A minishelterin Tpz1-Taz1 fusion protein bypasses requirement of Rap1 and Poz1 for replication-timing control and telomeric association of Taz1-dependent late origins

Previous studies have demonstrated that a minishelterin, an artificial fusion of Taz1 and Tpz1, is able to regulate telomere length in the absence of Rap1 and Poz1 (Pan *et al*, 2015). We examined whether a minishelterin Tpz1-Taz1 fusion protein restored replication-timing control in *rap1*Δ *poz1*Δ cells. BrdU incorporation was measured in *rap1*Δ *poz1*Δ double-mutant cells with or without expression of the Tpz1-Taz1 fusion protein (Fig 5A). In HU-treated *rap1*Δ *poz1*Δ cells, the Taz1-dependent late origins *AT2088* and *ori2100* replicated efficiently as the early origin *ars2004*, whereas the Taz1-independent late origin *ars727* and subtelomeric late origins *TAS59* and *tel-0.3* remained lower than non-origin control (Fig 5A). In contrast, early replication of *AT2088* and *ori2100* was suppressed by expression of the Tpz1-Taz1 fusion protein in *rap1*Δ *poz1*Δ cells (Fig 5A), indicating that the minishelterin restored replication-timing control of Taz1-dependent late origins. These results suggest that a link between Taz1 and Tpz1 is important for the replication-timing control of Taz1-dependent late origins located in the chromosome arm regions.

We examined whether the artificial fusion of Taz1 and Tpz1 also restored the telomeric association of internal late origins in the absence of Rap1 and Poz1. The distance between *AT2088*-LacI-GFP and the closest Taz1-mCherry during G1/S phase in *rap1*Δ *poz1*Δ double-mutant cells was significantly larger than in wild-type cells (Fig 5B and C). In contrast, expression of the Tpz1-Taz1 fusion protein decreased the distance between *AT2088*-LacI-GFP and the closest Taz1-mCherry locus in *rap1*Δ *poz1*Δ cells, such that it was similar to that of wild-type cells (Fig 5B and C). This indicated that the minishelterin restored telomeric localization of the Taz1-dependent late origin in the absence of Rap1 and Poz1. Contrastingly, expression of the minishelterin did not restore peripheral localization of *AT2088* in *rap1*Δ *poz1*Δ cells (Fig 5D), consistent with the notion that telomeric association of the internal Taz1-dependent late origin is independent of peripheral localization (Fig 3). These results suggest that the roles of Rap1 and Poz1 are to link Taz1 and Tpz1 in the shelterin complex and that the linkage is important for telomeric localization and replication-timing control of internal late origins.

Discussion

Replication origins on eukaryotic chromosomes are programed to initiate at specific timings during S phase (MacAlpine & Bell, 2005; Gilbert *et al*, 2010). In addition, replication takes place in distinct nuclear regions at specific timings, suggesting a link between temporal and spatial control of DNA replication. However, the biological significance of spatiotemporal replication and the molecular mechanisms behind its control are still unclear. In this study, we demonstrated that a subset of late replication origins regulated by Taz1 are confined to a specific intra-nuclear space, namely in proximity to telomeres in the nuclear periphery, during G1/S phase in fission yeast. Binding of Taz1 to the telomere-like sequences near the origins is essential for both the localization and the late-timing control of these origins, indicating that Taz1 plays a key role in linking the temporal and spatial regulation of chromosome replication.

In wild-type cells, Taz1-dependent late origins in chromosomal arm regions are predominantly located at the nuclear periphery (Fig 1) and near one of the telomeres during G1/S phase (Fig 2). Interestingly, the results in *bqt4*Δ cells, in which telomere anchoring to the inner nuclear membrane is disrupted, indicate that the telomere-adjacent localization and late-timing control are independent of the nuclear peripheral localization (Fig 3). Therefore, the peripheral localization itself is not a crucial determinant of late replication control, which is consistent with previous findings in budding yeast (Ebrahimi *et al*, 2010). In contrast, our study showed a strong correlation between telomere-adjacent localization and late-timing control of Taz1-dependent origins. Furthermore, the Taz1-dependent origin associates with the telomere when the replication program is established (Dimitrova & Gilbert, 1999). Taken together, our results suggest that telomere-adjacent localization plays an important role in replication-timing control of Taz1-dependent origins.

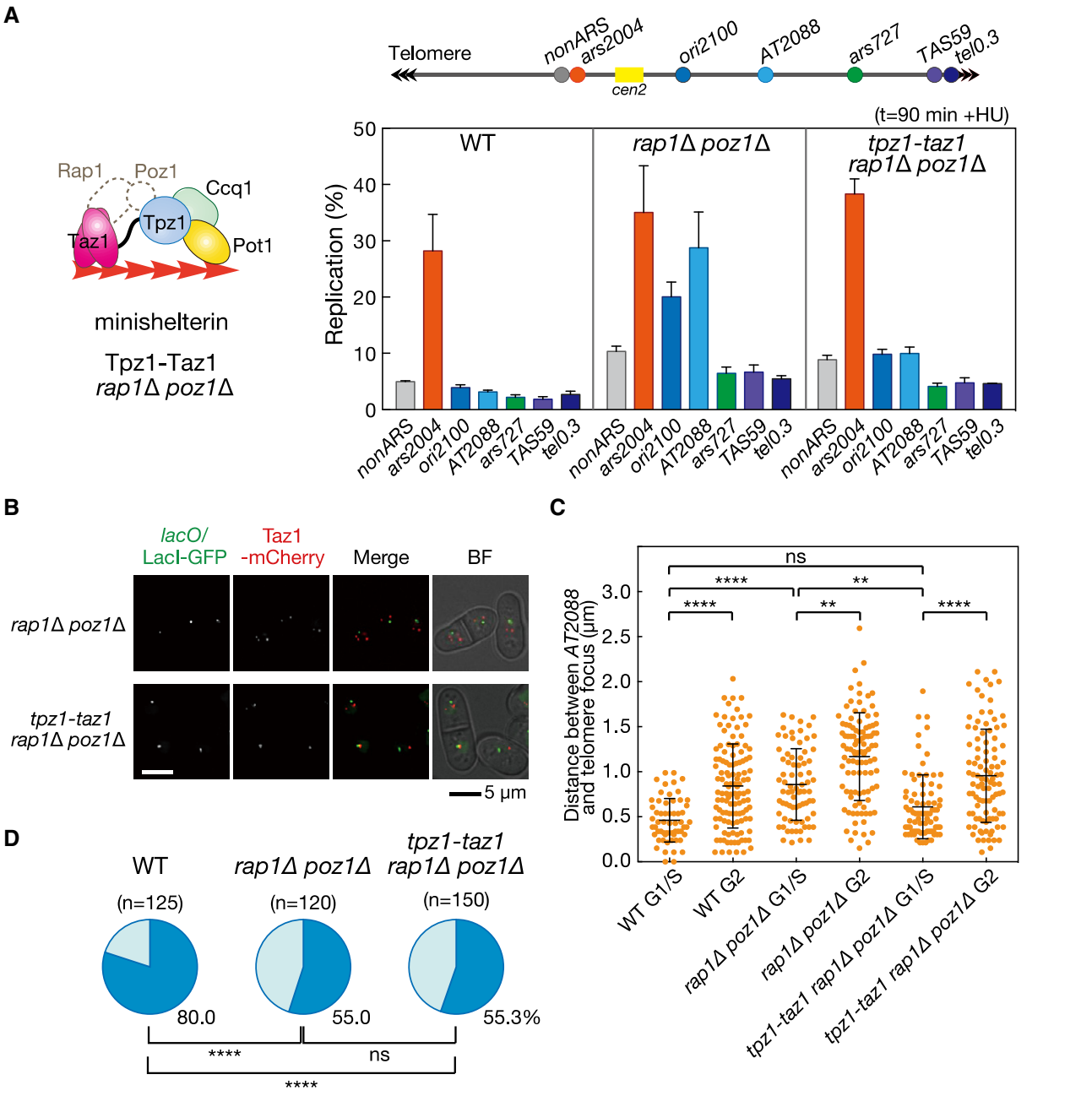

Figure 5. Minishelterin restores replication-timing control and telomeric association of Taz1-dependent late origins in the absence of Rap1 and Poz1.

A Effect of minishelterin expression on the replication timing of late origins. A minishelterin containing the Tpz1-Taz1 fusion protein is schematically presented. Wild-type and *rap1Δ poz1Δ* double-mutant cells with or without expression of the Tpz1-Taz1 fusion protein were synchronously released from the G2/M block and labeled with BrdU for 90 min in the presence of HU. Replication (%) was analyzed as described in Fig 3D. The mean values obtained from three independent experiments are presented ±SEM.

B Representative images are shown for *AT2088*-LacI-GFP in comparison with Taz1-mCherry in *rap1Δ poz1Δ* double-mutant cells with (bottom) or without (top) Tpz1-Taz1 expression. The scale bar indicates 5 μm.

C The distances between the *AT2088*-LacI-GFP focus and the closest Taz1-mCherry (telomere) in G1/S (n = 76) and G2 (n = 103) phases of *rap1Δ poz1Δ* cells and in G1/S (n = 82) and G2 (n = 99) phases of cells expressing the Tpz1-Taz1 fusion protein together with the results of wild-type cells (as in Fig 2) are shown in scatter plots. Lines indicate means ± SD. P-values were calculated using the Kruskal–Wallis test. ****P < 0.0001 and **P < 0.01.

D Localization of *AT2088*-LacI-GFP in comparison with Ish1-mCherry was analyzed in *rap1Δ poz1Δ* cells with or without expression of a Tpz1-Taz1 minishelterin. Class 1 (peripheral) and Class 2 (non-peripheral) proportions are shown in pie charts. P-values were calculated using Fisher's exact test. ****P < 0.0001.

We have previously shown that subtelomeric late origins replicate very late in the S phase in *S. pombe* (Hayashi *et al*, 2009). This is consistent with the model that Rif1 recruits PP1, which acts as a counter-phosphatase against the DDK-dependent phosphorylation of Mcm2-7 subunits and represses early replication (Hiraga *et al*, 2014). Thus, localization of Rif1 should be important for regulation

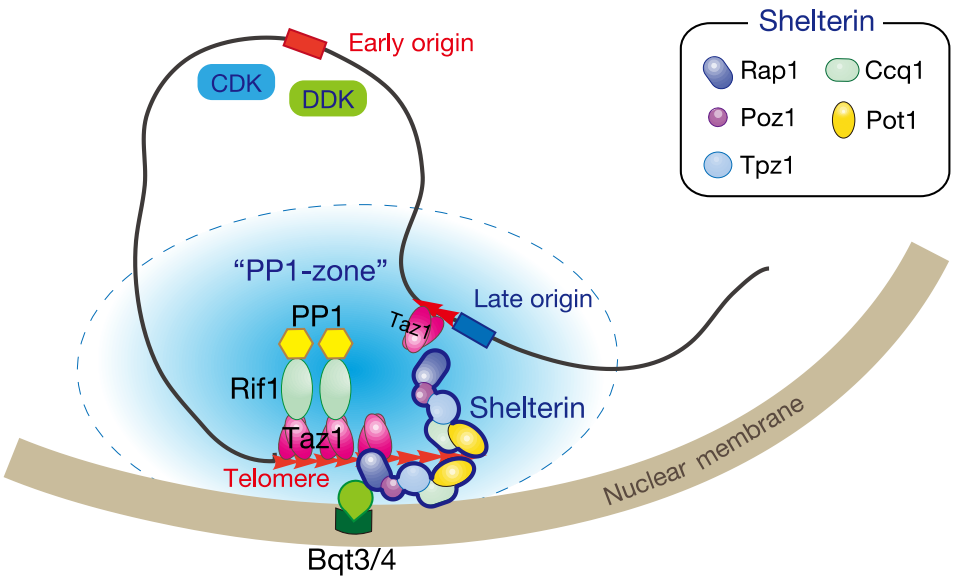

Figure 6. Model for replication-timing control by shelterin-mediated telomeric association.

A model for control of Taz1-dependent late origins by shelterin-mediated localization near the telomeres is shown. Taz1 binds to telomeric repeats (red arrowheads) at the telomeres, recruiting Rap1 and Rif1 to the telomeres. Telomeres are anchored to the nuclear membrane through the interaction of Rap1 with nuclear membrane protein Bqt3/4 during the interphase. Rif1 recruits PP1 that acts as a counter-phosphatase for DDK-phosphorylation of Mcm2-7 subunits. Subtelomeric late replication origins are strongly suppressed by PP1. Because Rif1 has a cloud-like localization around the telomeres (Appendix Fig S5), PP1 is likely to be enriched around telomeres, forming a "PP1-zone". Taz1 also binds to the telomere-like repeat (two arrowheads) near the replication origins in chromosomal arm regions throughout the cell cycle. During M phase, Taz1-bound origins as well as telomeres dissociate from the nuclear membrane. At the end of M phase, Taz1-bound origins associate with telomeres, possibly through interaction of Taz1 with the shelterin component Rap1. During G1/S phase, telomeres are anchored to the nuclear membrane, and Taz1-dependent origins tethered around the telomeres are suppressed by PP1.

of replication timing. Interestingly, Rif1-EGFP exhibits a cloud-like tailed localization around a defined focus of Taz1-mCherry in G1/S cells (Appendix Fig S5), as reported previously (Zaaijer *et al*, 2016). It is possible that PP1 is enriched around the telomeres forming a phosphatase dominant "PP1-zone" (Fig 6). Thus, tethering of Taz1-dependent origins to telomeres during G1/S phase may inhibit replication initiation through PP1 until DDK and CDK activities increase in late S phase (Fig 6). This implies that adjacent regions to the telomere-like sequence would be inhibited by the PP1-zone. Indeed, the average distance of a Taz1-dependent late origin to the nearest early origin (67 kb) is much larger than the average distance between early origins (27 kb), based on the previous results (Tazumi *et al*, 2012), supporting the idea.

Shelterin components Rap1 and Poz1 are required for telomeric association and replication-timing control of Taz1-dependent late origins located in chromosomal arm regions (Fig 4). Interestingly, neither Rap1 nor Poz1 is required for the control of subtelomeric late origins near the telomeres (Fig 4), suggesting that Rap1 and Poz1 have a specific role in regulation of telomere-distal origins. Because Rap1 and Poz1 are components of the shelterin complex that forms a physical bridge connecting Taz1 and Pot1 at the telomeres (Miyoshi *et al*, 2008; Palm & de Lange, 2008), it is possible that they contribute to tethering Taz1-bound internal origins to the telomeres (Fig 6). Indeed, the requirement of Rap1 and Poz1 for both timing control and telomeric association of the internal late origin was bypassed by expression of a minishelterin Tpz1-Taz1 fusion protein (Fig 5), consistent with the importance of the physical linkage of shelterin in replication-timing control. Furthermore, timing control of the internal late origins under the expression of the minishelterin in the absence of Rap1 and Poz1 still requires Rif1 (Appendix Fig S6), suggesting that certain physical inaccessibility of initiation factors due to the Tpz1-Taz1 fusion protein is unlikely. In addition, tethering of LacI-GFP-Sds21/PP1 phosphatase to the *lacO* repeat proximal to *AT2088* in *rap1*Δ cells decreased early replication of *AT2088* (Appendix Fig S7), suggesting that requirement of Rap1 in timing control was, at least partly, bypassed by localization of PP1 to the origin. These results are consistent with the model that telomere-adjacent localization causes repression of Taz1-dependent late origins, although the involvement of other mechanisms dependent on Rif1 and PP1 cannot be excluded.

Recent studies using chromosome conformation capture (3C) or Hi-C techniques have revealed that chromatin units in spatial proximity, known as topologically associated domains (TADs), influence transcription and DNA replication (Dileep *et al*, 2015; Gonzalez-Sandoval & Gasser, 2016). The close association of Taz1-dependent late origins with the telomeres described in the present study may represent a novel type of TAD that is formed transiently during G1/S phase. It is possible that this type of TAD contributes to formation of facultative heterochromatin around Taz1-dependent late origins, although deletion of heterochromatin protein HP1 only marginally affected replication-timing control (Zofall *et al*, 2016). The actual topological association between the chromosome arm regions and telomeres was not detected in wild-type cells, but was

detected in the mutant cells of a chromatin-associated protein Sap1 (Mizuguchi *et al*, 2017). This was probably due to a transient interaction between internal late origins and telomeres during G1/S phase. A cell cycle-specific investigation may be needed to study this interaction.

In the present study, we demonstrated that telomere-like sequences and telomere-binding proteins play important roles in intra-nuclear localization and replication-timing control of a subset of late replication origins. In addition, the results obtained in this study uncovered novel functions of telomeres in higher order chromatin architectures and long-distance control of DNA replication. Although the mechanisms involved in replication-timing control might be diverse in various organisms, localization of origins to specific nuclear compartment may play roles in control of the initiation process. Because telomeric sequences and telomere-binding proteins are widely conserved in eukaryotes, investigation on the functions of these features in various organisms would shed light on our understanding of roles of intra-nuclear compartments in chromosomal functions, including gene expression, DNA replication, DNA damage repair, and genome maintenance.

Materials and Methods

Yeast strains, media, and transformations

The *Schizosaccharomyces pombe* strains used in this study are listed in Appendix Table S1. Yeast cells were grown in YE medium as a complete medium and EMM medium as a minimum medium (Moreno *et al*, 1991), supplemented with 2% glucose and appropriate nutrients. Transformation of *S. pombe* was performed using the lithium acetate method (Forsburg, 2003), and transformants were selected on solid YE medium containing 2% agar supplemented with appropriate antibiotics, such as geneticin (G418, Nacalai Tesque), hygromycin B (Nacalai Tesque), and nourseothricin (clonNAT, Werner BioAgents), at a final concentration of 100 μg/ml.

Visualization of replication origin loci

Replication origin loci were visualized using a *lac* operator (*lacO*)/GFP-conjugated *lac* repressor (LacI) system (Robinett *et al*, 1996; Straight *et al*, 1996). The LacI protein constructed in Nabeshima *et al* (1998) was used in this study; 256 tandem arrays of *lacO* repeats were integrated at a site 100–700 bp from the replication origin using the two-step integration method (Yamamoto & Hiraoka, 2003). First, a DNA fragment containing a partial *ura4* gene was integrated at the targeted locus, and the *lacO* tandem repeats were subsequently integrated at the locus, thus generating the *ura4*$^+$ sequence. To integrate the partial *ura4* gene at the early or late origin, pCT33 h was constructed by replacing the *Mlu*I-*Sac*I fragment containing the kanamycin-resistant (*kanMX6*) gene of pCT33-6 with the *Mlu*I-*Sac*I fragment containing the hygromycin-resistant (*hphMX6*) gene from pFA6a-hphMX6. Subsequently, a DNA fragment containing both the partial *ura4* gene and the *hphMX6* gene was amplified by PCR using two DNA primers from pCT33 h. The primers used to amplify pCT33 h are listed in Appendix Table S2. Integration of the amplified DNA fragment was executed at a targeted origin locus of LacI-GFP-carrying cells (HM5833: *h*$^+$ *his7*$^+$::*lacI-GFP lys1-131 ura4-D18*), which was obtained by standard genetic crosses between HM643 and YHS119. pCT31-13 containing the *lacO* tandem repeats was linearized by *Stu*I and introduced into the cell line containing the partial *ura4* gene at the target site. Ura$^+$ transformants were selected, and the insertion of *lacO* repeats was confirmed by PCR.

A fission yeast strain expressing Ish1-mCherry and LacI-GFP was obtained using standard genetic crosses between HMP16 and HM5833, resulting in HM5632. To construct the strain expressing Taz1-mCherry, two short fragments were amplified by PCR from the genomic DNA of *S. pombe* wild-type strain 972 using two sets of primers, #1744 and #3069; and #3042 and #1776 (Appendix Table S2). The products were used as primers for the amplification of *taz1-mCherry-kan* from pFA6a-mCherry-kanMX6. The PCR products were used for integrating at the *taz1*$^+$ locus, and G418-resistant transformants were selected.

Construction of fission yeast strains

HM3488, HM5023, HM5189, HM5760, HM5790, and HM5990, derivatives carrying *cdc25-22* P_{nmt1}*-TK* P_{adh1}*-hENT*, were obtained by standard genetic crossing. The *ish1-mCherry taz1*Δ derivatives were generated using standard genetic crossing of HM5731, HM5541, HM5726, or HM5688 with HM5027.

For construction of the *bqt4*Δ strain, a 3.9-kb fragment containing the *bqt4*$^+$ gene was amplified by PCR from the genomic DNA of wild-type strain 972 using the primers #3542 and #3543. Then, the upstream region amplified from the 3.9-kb fragment using primers #3548 and #3549 was digested by *Hin*dIII and *Sal*I and cloned into the *Hin*dIII-*Sal*I sites of pFA6a-natMX6 to generate pBQ5′. Next, the downstream region of the *bqt4*$^+$ gene was amplified from the 3.9-kb fragment using the primers #3550 and #3551, digested by *Sac*I and *Eco*RV, and then cloned into the *Sac*I-*Eco*RV sites of pBQ5′, resulting in pFA6a-Bqt4d-natMX6. The *Sac*I-*Eco*RV fragment of pFA6a-Bqt4d-natMX6 was used for transformation of HM5805 and HM5541, resulting in HM5835 and HM6022, respectively.

For construction of the minishelterin *tpz1-taz1 rap1*Δ *poz1*Δ strain, the artificial *tpz1-poz1* fusion gene was amplified by PCR from the genomic DNA of the PP993 strain using primers #3575 and #3576, and used for transformation of HM5790, resulting in HM5991. The derivatives of *taz1-mCherry* carrying *rap1*Δ or *poz1*Δ were constructed by standard genetic crossing of HM5805 with HM5025 resulting in HM5860, and HM5805 with HM3578 resulting in HM5861.

Live cell imaging

Schizosaccharomyces pombe cells grown in YE medium at 30°C to 1×10^7 cells/ml were immobilized on a glass-bottom dish (MatTek Corp.) coated with lectin (0.2 mg/ml, Sigma) in EMM medium. A DeltaVision Elite fluorescence microscopy system (GE Healthcare Life Science), which is based on an Olympus wide-field IX71 fluorescence microscope and equipped with a CoolSNAP HQ2 CCD camera (Photometrics), was used for live cell imaging. Live cell images were obtained using an oil-immersion objective lens (Plan Apo 60×; NA = 1.4; Olympus) at 30°C in a temperature-controlled room.

Optical section images were processed with 3D deconvolution and analyzed using the SoftWoRx 5.5 software on the DeltaVision Elite system (GE Healthcare Life Science).

BrdU incorporation and replication timing analysis

HM1865, HM3488, HM5023, HM5189, HM5769, or HM 5932 cells carrying P_{nmt1}-*TK* P_{adh1}-*hENT cdc25-22* were grown in EMM medium lacking thiamine to induce transcription of the TK gene at 25°C (1×10^7 cells/ml). Cells were further incubated at 36°C for 3 h to arrest at the G2/M boundary due to the *cdc25-22* mutation, and the cell cycle was synchronously restarted at 25°C in the presence of 200 μM BrdU and 10 mM HU for 90 min. The preparation of cellular DNA and separation of BrdU-labeled DNA from unreplicated DNA by CsCl density gradient centrifugation were carried out as previously described (Hayashi *et al*, 2007). The amount of DNA in the heavy–light and light–light densities was analyzed using qPCR with the primers listed in Appendix Table S2.

Chromatin immunoprecipitation assay

ChIP assays were performed as described previously (Handa *et al* 2012). Immunoprecipitation was conducted using Dynal magnetic beads (Invitrogen) associated with mouse anti-FLAG (1:500, M2 monoclonal; Sigma). The immunoprecipitated and total DNAs were quantitated by qPCR with SYBR green 1 in Applied Biosystems StepOne real-time PCR system (Life technologies). The primers used for qPCR are listed in Appendix Table S2.

Statistical analysis

Statistical analysis was performed using the Fisher's exact test for independence of two nominal variables with small sample sizes to compare the nuclear peripheral localization, or using the Kruskal–Wallis test, a non-parametric method for testing whether samples originate from the same distribution, to compare telomere association in "GraphPad Prism 6" (GraphPad Software, Inc.), with $P < 0.05$ considered as significant. The middle bar indicates the mean distance between the LacI-GFP and the closest Taz1-mCherry foci, and the top and bottom bars indicate SD.

Expanded View for this article is available online.

Acknowledgements
We thank Drs. Peter Baumann, Fuyuki Ishikawa, and Junko Kanoh for providing the plasmids and yeast strains and Drs. Hiroyuki Araki, Makoto Hayashi, and My Khanh Pham for critical reading of the manuscript. This study was supported by a Grant-in-Aid from the Ministry of Education, Culture, Sports, Science, and Technology of Japan to HM.

Author contributions
SO, TST, TN, YH, and HM participated in the design of the study. SO, SK, TH, and HM participated in molecular genetic and molecular imaging studies. SO, HO, HA, and YH contributed to analysis and interpretation of the fluorescent microscope images in YH laboratory. SO and HM drafted the manuscript, and HM participated in coordination of the study. All authors read and approved the final manuscript.

Conflict of interest
The authors declare that they have no conflict of interest.

References

Chikashige Y, Tsutsumi C, Yamane M, Okamasa K, Haraguchi T, Hiraoka Y (2006) Meiotic proteins bqt1 and bqt2 tether telomeres to form the bouquet arrangement of chromosomes. *Cell* 125: 59 – 69

Chikashige Y, Yamane M, Okamasa K, Tsutsumi C, Kojidani T, Sato M, Haraguchi T, Hiraoka Y (2009) Membrane proteins Bqt3 and -4 anchor telomeres to the nuclear envelope to ensure chromosomal bouquet formation. *J Cell Biol* 187: 413 – 427

Chikashige Y, Haraguchi T, Hiraoka Y (2010) Nuclear envelope attachment is not necessary for telomere function in fission yeast. *Nucleus* 1: 481 – 486

Cooper JP, Nimmo ER, Allshire RC, Cech TR (1997) Regulation of telomere length and function by a Myb-domain protein in fission yeast. *Nature* 385: 744 – 747

Crabbe L, Cesare AJ, Kasuboski JM, Fitzpatrick JA, Karlseder J (2012) Human telomeres are tethered to the nuclear envelope during postmitotic nuclear assembly. *Cell Rep* 2: 1521 – 1529

Dave A, Cooley C, Garg M, Bianchi A (2014) Protein phosphatase 1 recruitment by Rif1 regulates DNA replication origin firing by counteracting DDK activity. *Cell Rep* 7: 53 – 61

Dileep V, Rivera-Mulia JC, Sima J, Gilbert DM (2015) Large-scale chromatin structure-function relationships during the cell cycle and development: insights from replication timing. *Cold Spring Harb Symp Quant Biol* 80: 53 – 63

Dimitrova DS, Gilbert DM (1999) The spatial position and replication timing of chromosomal domains are both established in early G1 phase. *Mol Cell* 4: 983 – 993

Ebrahimi H, Robertson ED, Taddei A, Gasser SM, Donaldson AD, Hiraga S (2010) Early initiation of a replication origin tethered at the nuclear periphery. *J Cell Sci* 123: 1015 – 1019

Ferreira HC, Towbin BD, Jegou T, Gasser SM (2013) The shelterin protein POT-1 anchors *Caenorhabditis elegans* telomeres through SUN-1 at the nuclear periphery. *J Cell Biol* 203: 727 – 735

Forsburg SL (2003) Introduction of DNA into *S. pombe* cells. *Curr Protoc Mol Biol* Chapter 13: Unit 13 17

Gilbert DM, Takebayashi SI, Ryba T, Lu J, Pope BD, Wilson KA, Hiratani I (2010) Space and time in the nucleus: developmental control of replication timing and chromosome architecture. *Cold Spring Harb Symp Quant Biol* 75: 143 – 153

Gonzalez-Sandoval A, Gasser SM (2016) On TADs and LADs: spatial control over gene expression. *Trends Genet* 32: 485 – 495

Handa T, Kanke M, Takahashi TS, Nakagawa T, Masukata H (2012) DNA polymerization-independent functions of DNA polymerase epsilon in assembly and progression of the replisome in fission yeast. *Mol Biol Cell* 23: 3240 – 3253

Hayano M, Kanoh Y, Matsumoto S, Renard-Guillet C, Shirahige K, Masai H (2012) Rif1 is a global regulator of timing of replication origin firing in fission yeast. *Genes Dev* 26: 137 – 150

Hayashi M, Katou Y, Itoh T, Tazumi A, Yamada Y, Takahashi T, Nakagawa T, Shirahige K, Masukata H (2007) Genome-wide localization of pre-RC sites and identification of replication origins in fission yeast. *EMBO J* 26: 1327 – 1339

Hayashi MT, Takahashi TS, Nakagawa T, Nakayama J, Masukata H (2009) The heterochromatin protein Swi6/HP1 activates replication origins at the

pericentromeric region and silent mating-type locus. *Nat Cell Biol* 11: 357 – 362

Heun P, Laroche T, Raghuraman MK, Gasser SM (2001) The positioning and dynamics of origins of replication in the budding yeast nucleus. *J Cell Biol* 152: 385 – 400

Hiraga S, Alvino GM, Chang F, Lian HY, Sridhar A, Kubota T, Brewer BJ, Weinreich M, Raghuraman MK, Donaldson AD (2014) Rif1 controls DNA replication by directing Protein Phosphatase 1 to reverse Cdc7-mediated phosphorylation of the MCM complex. *Genes Dev* 28: 372 – 383

Kanoh J, Ishikawa F (2001) spRap1 and spRif1, recruited to telomeres by Taz1, are essential for telomere function in fission yeast. *Curr Biol* 11: 1624 – 1630

Kanoh Y, Matsumoto S, Fukatsu R, Kakusho N, Kono N, Renard-Guillet C, Masuda K, Iida K, Nagasawa K, Shirahige K, Masai H (2015) Rif1 binds to G quadruplexes and suppresses replication over long distances. *Nat Struct Mol Biol* 22: 889 – 897

MacAlpine DM, Bell SP (2005) A genomic view of eukaryotic DNA replication. *Chromosome Res* 13: 309 – 326

Mattarocci S, Shyian M, Lemmens L, Damay P, Altintas DM, Shi T, Bartholomew CR, Thoma NH, Hardy CF, Shore D (2014) Rif1 controls DNA replication timing in yeast through the PP1 phosphatase Glc7. *Cell Rep* 7: 62 – 69

Miyoshi T, Kanoh J, Saito M, Ishikawa F (2008) Fission yeast Pot1-Tpp1 protects telomeres and regulates telomere length. *Science* 320: 1341 – 1344

Mizuguchi T, Taneja N, Matsuda E, Belton JM, FitzGerald P, Dekker J, Grewal SIS (2017) Shelterin components mediate genome reorganization in response to replication stress. *Proc Natl Acad Sci USA* 114: 5479 – 5484

Moreno S, Klar A, Nurse P (1991) Molecular genetic analysis of fission yeast *Schizosaccharomyces pombe*. *Methods Enzymol* 194: 795 – 823

Nabeshima K, Nakagawa T, Straight AF, Murray A, Chikashige Y, Yamashita YM, Hiraoka Y, Yanagida M (1998) Dynamics of centromeres during metaphase-anaphase transition in fission yeast: Dis1 is implicated in force balance in metaphase bipolar spindle. *Mol Biol Cell* 9: 3211 – 3225

Nakamura H, Morita T, Sato C (1986) Structural organizations of replicon domains during DNA synthetic phase in the mammalian nucleus. *Exp Cell Res* 165: 291 – 297

Nakayasu H, Berezney R (1989) Mapping replicational sites in the eucaryotic cell nucleus. *J Cell Biol* 108: 1 – 11

O'Keefe RT, Henderson SC, Spector DL (1992) Dynamic organization of DNA replication in mammalian cell nuclei: spatially and temporally defined replication of chromosome-specific alpha-satellite DNA sequences. *J Cell Biol* 116: 1095 – 1110

Palladino F, Laroche T, Gilson E, Axelrod A, Pillus L, Gasser SM (1993) SIR3 and SIR4 proteins are required for the positioning and integrity of yeast telomeres. *Cell* 75: 543 – 555

Palm W, de Lange T (2008) How shelterin protects mammalian telomeres. *Annu Rev Genet* 42: 301 – 334

Pan L, Hildebrand K, Stutz C, Thoma N, Baumann P (2015) Minishelterins separate telomere length regulation and end protection in fission yeast. *Genes Dev* 29: 1164 – 1174

Robinett CC, Straight A, Li G, Willhelm C, Sudlow G, Murray A, Belmont AS (1996) *In vivo* localization of DNA sequences and visualization of large-scale chromatin organization using lac operator/repressor recognition. *J Cell Biol* 135: 1685 – 1700

Spink KG, Evans RJ, Chambers A (2000) Sequence-specific binding of Taz1p dimers to fission yeast telomeric DNA. *Nucleic Acids Res* 28: 527 – 533

Straight AF, Belmont AS, Robinett CC, Murray AW (1996) GFP tagging of budding yeast chromosomes reveals that protein-protein interactions can mediate sister chromatid cohesion. *Curr Biol* 6: 1599 – 1608

Taricani L, Tejada ML, Young PG (2002) The fission yeast ES2 homologue, Bis1, interacts with the Ish1 stress-responsive nuclear envelope protein. *J Biol Chem* 277: 10562 – 10572

Tazumi A, Fukuura M, Nakato R, Kishimoto A, Takenaka T, Ogawa S, Song JH, Takahashi TS, Nakagawa T, Shirahige K, Masukata H (2012) Telomere-binding protein Taz1 controls global replication timing through its localization near late replication origins in fission yeast. *Genes Dev* 26: 2050 – 2062

Yamamoto A, Hiraoka Y (2003) Monopolar spindle attachment of sister chromatids is ensured by two distinct mechanisms at the first meiotic division in fission yeast. *EMBO J* 22: 2284 – 2296

Zaaijer S, Shaikh N, Nageshan RK, Cooper JP (2016) Rif1 regulates the fate of DNA entanglements during mitosis. *Cell Rep* 16: 148 – 160

Zofall M, Smith DR, Mizuguchi T, Dhakshnamoorthy J, Grewal SI (2016) Taz1-shelterin promotes facultative heterochromatin assembly at chromosome-internal sites containing late replication origins. *Mol Cell* 62: 862 – 874